Possible physical realizations of the Tolman VII solution

Ambrish M. Raghoonundun* and David W. Hobill†
University of Calgary, 2500 University Drive NW, Calgary, Alberta, Canada, T2N 1N4

The Tolman VII solution for a static perfect fluid sphere to the Einstein equations is reexamined, and a closed form class of equations of state (EOSs) is deduced for the first time. These EOSs allow further analysis to be carried out, leading to a viable model for compact stars with arbitrary boundary mass density to be obtained. Explicit application of causality conditions places further constraints on the model, and recent observations of masses and radii of neutron stars prove to be within the predictions of the model. The adiabatic index predicted is $\gamma \geq 2$, but self-bound crust solutions are not excluded if we allow for higher polytropic indices in the crustal regions of the star. The solution is also shown to obey known stability criteria often used in modeling such stars. It is argued that this solution provides realistic limits on models of compact stars, maybe even independently of the type of EOS, since most of the EOSs usually considered do show a quadratic density falloff to first order, and this solution is the unique exact solution that has this property.

PACS numbers: 04.20.Jb, 04.40.Dg, 95.30.Sf, 97.60.Jd

I. INTRODUCTION

The construction of exact analytic solutions to the Einstein equations has had a long history, nearly one hundred years to be more precise. However, in spite of the fact that the total number of solutions is large [1] and growing, only a small subset of those solutions can be thought of as having any physical relevance. Most solutions exhibit mathematical pathologies or violate simple principles of physics (energy conditions, causality, etc.) and are therefore not viable descriptions of any observable or potentially observable phenomena.

Indeed, works that review exact solutions and their properties demonstrate the difficulties associated with constructing solutions that might be relevant to gravitating systems that actually exist in our Universe. Even in the simplest case of exact analytic solutions for static, spherically symmetric fluid spheres, it has been shown that less than ten percent of the many known solutions can be considered as describing a realistic, observable object. For example, Delgaty and Lake, using computer algebra methods, reviewed over 130 solutions and found that only nine could be classified as physically relevant [2]. A similar study by Finch and Skea arrived at the same conclusion [3]. The latter review also introduced an additional criterion that further reduced the number of physically relevant solutions to those that have exact analytic equations of state (EOSs) of the form $p = p(\rho)$, where p is the fluid pressure and ρ is the matter density. This class of solutions was called "the set of interesting solutions."

In 1939 Tolman introduced a technique for constructing solutions to the static, spherically symmetric Einstein equations with material fluid sources [4]. That method led to eight exact analytic expressions for the metric functions, the matter density and in some cases the fluid pressure. Beginning with an exact analytic solution for one of the two metric functions, an expression for the mass density could be obtained by integration. With expressions for the density and the first metric function in hand, an analytic expression for the second metric function could be obtained. This often required an appropriate change of the radial variable to obtain a simple integral. All functions could then be written as explicit functions of the radial coordinate r. While the fluid pressure could, in principle, be obtained from the metric and density functions, Tolman chose not to evaluate the fluid pressure in some cases due to the fact that to do so would lead to mathematically rather complicated expressions that might be difficult to interpret.

Of the eight solutions presented in his paper, three were already known (the Einstein universe, the Schwarzschild–de Sitter solution, and the Schwarzschild constant density solution); most of the others "describe situations which are frankly unphysical, and these do have a tendency to distract attention from the more useful ones." [5]. One, the so-called Tolman VII solution appeared to have some physical relevance, but this was one of the solutions for which no explicit expression for the pressure was given.

The Tolman VII solution has been rediscovered a number of times and has appeared under different names, the Durgapal [6, 7] and the Mehra solutions being two examples. That these solutions can be used to describe realistic physical systems has been noted by many authors, including those of the two review papers mentioned above [2, 3]. It has been used as an exact analytic model for spherically symmetric stellar systems, and additional research has investigated its stability properties [9, 10]. While these later works were able to obtain the complicated expressions for the fluid pressure as a function of the radial coordinate, according to Finch and Skea [3] it still was not one of the "interesting solutions" since it lacked an explicit expression for the equation of state. The choice of parameters that has been taken by differ-

* amraghoo@ucalgary.ca
† hobill@ucalgary.ca

ent authors in order to completely specify the solution in many ways prevented the immediate interpretation of the physical conditions described by the solution.

The reasons mentioned above are not sufficient to use or classify the Tolman VII solution as a physically viable one. Instead, we seek physical motivations for the viability of this solution, and indeed we find these in many forms:

(i) From a Newtonian point of view, simple thermodynamic arguments yield polytropes of the form $p(\rho) = k\rho^\gamma$ (here γ is the adiabatic index sometimes written in terms of the polytropic index n, $\gamma = 1 + 1/n$, and k is known at the adiabatic constant that can vary from star to star) as viable models for neutron matter. When coupled with Newtonian hydrodynamic stability and gravitation, the result is the Lane-Emden differential equation for the density profile, $\rho(r)$. Solutions of the latter, obtained numerically, or in particular cases ($\gamma = \infty, 2$, or 1.2) exactly, all have a distinctive density falloff from the center to the edge of the Newtonian star. This is a feature we wish physical solutions to have. Furthermore, this distinctive falloff is quadratic in the rescaled radius [11], suggesting that even in the relativistic case, such a falloff would be a good first approximation to model realistic stars, which have a proper thermodynamic grounding.

(ii) Looking at viable exact relativistic solutions to the Einstein equations, the one used extensively before 1939 and even much later, was the Schwarzschild interior solution. This solution has the feature that the density is constant throughout the sphere, and is not physical: the speed of sound (pressure) waves in its interior is infinite. However, this solution provides clear predictions about the maximum possible mass of relativistic stars in the form of the Buchdahl limit [12]: $M \leq 4R/9$. The next best guess in this line of reasoning of finding limiting values from exact solutions would be to find an exact solution with a density profile that decreases with increasing radius, since a stability heuristic for stars demands that $\mathrm{d}\rho/\mathrm{d}r \leq 0$, as expected from (i) in the Newtonian case. Extension to the relativistic Lane-Emden equation also requires [11] that $(\mathrm{d}\rho/\mathrm{d}r)|_{r=0} = 0$, a property Tolman VII has.

(iii) Additionally, an extensive review [13] of most EOSs used from nuclear physics to model neutron stars concluded that a quadratic falloff in the density is a very close approximation to *most* such nuclear models–the differences of drastically different nuclear models from Tolman VII being only minor if only the density profiles were compared. Since Tolman VII is precisely the unique exact solution to the full Einstein field equations that exhibits a quadratic falloff in the density profile, we believe that it captures much of what nuclear models have to say about the overall structure of relativistic stars.

These three reasons taken together make a strong case for considering the Tolman VII solution as the best possible exact solution that is capable of describing a wide class of EOSs for neutron stars. At the very least, it is as good a candidate that captures first-order effects in density of *most* nuclear model EOSs, and at best it is the model that all realistic nuclear models tend to, while including features like self-boundedness naturally, as we shall show.

The purpose of this paper is to reexamine the Tolman VII solution by introducing a set of constant parameters that we believe provide a more intuitive understanding of the physical content of the solution. In addition, the solution now becomes a member of the set of "interesting solutions" since we provide an explicit expression for a class of equations of state derived from the solution without any further assumptions about the matter, except for the Newtonian-like, and physically motivated quadratic falloff of the density. The EOSs will allow for further exploration of the predictions of the solution as well as a description of the material that makes up the star. The imposition of both the causality conditions where the speed of sound in the fluid never exceeds the speed of light and the different boundary conditions will provide further restrictions on the parameters associated with the solution. What this all leads to is a complete analytic model for compact stars that can be used to compare with recent observations of neutron star masses and radii. That the Tolman VII solution is consistent with all observations of astrophysical neutron stars leads to the conclusion that this exact solution is physically relevant while having features present in compact objects found in nature.

This article is divided as follows: following a brief historical introduction in Sec. I, we re-derive the Tolman VII solution in Sec. II, paying particular attention to the pressure expression with physically more intuitive variables. We then invert the density equation and use the pressure expression just found to derive a class of EOSs in Sec. III, where we also carry out an analysis of the said class of EOSs. In the same section, we contrast the two different types of physical models that the solution admits, and we shall also show how qualitative differences arise in the stars' structure and quantitative ones appear in the predicted values of the adiabatic indices of the fluid. Finally we provide some brief concluding remarks in Sec. IV.

II. THE TOLMAN VII SOLUTION

Beginning with a line element in terms of standard areal (Schwarzschild) coordinates for a static and spherically symmetric metric,

$$\mathrm{d}s^2 = \mathrm{e}^{\nu(r)}\mathrm{d}t^2 - \mathrm{e}^{\lambda(r)}\mathrm{d}r^2 - r^2\mathrm{d}\theta^2 - r^2\sin^2\theta\mathrm{d}\varphi^2, \quad (1)$$

the Einstein equations for a perfect fluid source lead to three ordinary differential equations for the two metric variables ν, λ, and the two matter variables ρ and p.

However, these variables will not be the most practical ones to carry out our analysis. Instead two related metric functions, $Z(r) = \mathrm{e}^{-\lambda(r)}$ and $Y(r) = \mathrm{e}^{\nu(r)/2}$, are introduced, as prescribed in Ivanov [14]. The reason for introducing these new metric variables is that with the assumption made for the density function, these variables will transform the original nonlinear differential equations into linear ones which may then be easily solved.

Given the metric equation (1), the Einstein equations reduce to the following set of three coupled ordinary differential equations (ODEs) for the four variables Z, Y, p, and ρ:

$$\kappa\rho = \mathrm{e}^{-\lambda}\left(\frac{\lambda'}{r} - \frac{1}{r^2}\right) + \frac{1}{r^2} = \frac{1}{r^2} - \frac{Z}{r^2} - \frac{1}{r}\frac{\mathrm{d}Z}{\mathrm{d}r}, \tag{2a}$$

$$\kappa p = \mathrm{e}^{-\lambda}\left(\frac{\nu'}{r} + \frac{1}{r^2}\right) - \frac{1}{r^2} = \frac{2Z}{rY}\frac{\mathrm{d}Y}{\mathrm{d}r} + \frac{Z}{r^2} - \frac{1}{r^2}, \tag{2b}$$

$$\kappa p = \mathrm{e}^{-\lambda}\left(\frac{\nu''}{2} - \frac{\nu'\lambda'}{4} + \frac{(\nu')^2}{4} + \frac{\nu' - \lambda'}{2r}\right) = \frac{Z}{Y}\frac{\mathrm{d}^2Y}{\mathrm{d}r^2} + \frac{1}{2Y}\frac{\mathrm{d}Y}{\mathrm{d}r}\frac{\mathrm{d}Z}{\mathrm{d}r} + \frac{Z}{rY}\frac{\mathrm{d}Y}{\mathrm{d}r} + \frac{1}{2r}\frac{\mathrm{d}Z}{\mathrm{d}r}. \tag{2c}$$

where the primes ($'$) denote differentiation with respect to r, and κ is equal to 8π, since in what follows natural units where $G = c = 1$ are introduced.

The first two equations (2a) and (2b) can be added together to generate the simpler equation

$$\kappa(p + \rho) = \frac{2Z}{rY}\frac{\mathrm{d}Y}{\mathrm{d}r} - \frac{1}{r}\frac{\mathrm{d}Z}{\mathrm{d}r}, \tag{3}$$

which will be useful later on. In order to solve this set of ODEs, one begins with equation (2a) and assumes a specific functional form for the density, one that is motivated from physical considerations according to (iii). Since this is a linear inhomogeneous ODE for $Z(r)$, one can for the appropriately chosen form of $\rho(r)$ easily integrate this equation. The Tolman VII density has a simple functional form:

$$\rho = \rho_c\left[1 - \mu\left(\frac{r}{r_b}\right)^2\right], \tag{4}$$

where the constant r_b represents the boundary radius as mentioned previously, ρ_c represents the central density at $r = 0$, and μ is a "self-boundedness" dimensionless parameter that spans values between 0 and 1, so that when it is equal to 0, we have a sphere of constant density, and when it is equal to 1, we have a "natural" star, with density vanishing at the boundary.

Although very simple, this quadratic function is known to provide a good approximation for the density profile of a number of neutron star's EOSs. For example, Fig 5 in Ref. [13] plots the density profile of 12 EOSs and compares them to a function of the form given in equation (4) (for the $\mu = 1$ case). Therefore, the claim is that this functional form is a generic feature of many different types of nuclear EOSs and this suggests that at the very least some global features of such a density profile might describe the bulk properties of many compact objects.

The set of three parameters that describe the density function will occur frequently in what follows and will be denoted as: $\mathbf{\Pi} \coloneqq \{\rho_c, r_b, \mu\}$. The form of the density function for $\mu > 0$ is physically realistic, since it is monotonically decreasing from the center to the edge of the sphere, as argued previously in (ii) and (iii), in contrast to the constant-density exact solution frequently used to model such objects.

Additionally, boundary conditions are required for the system, since we eventually want to match this interior solution to an external metric. Since the vacuum region is spherically symmetric and static, the only candidate by Birkhoff's theorem is the Schwarzschild exterior solution. The Israel-Darmois junction conditions for this system can then be shown to be equivalent to the following two conditions [15]:

$$p(r_b) = 0, \quad \text{and} \tag{5a}$$

$$Z(r_b) = 1 - \frac{2M}{r_b} = Y^2(r_b), \tag{5b}$$

where $M = m(r_b)$ is the total mass of the sphere as seen by an outside observer, and $m(r)$ is the mass function defined by

$$m(r) = 4\pi\int_0^r \rho(\bar{r})\bar{r}^2\mathrm{d}\bar{r}. \tag{6}$$

Furthermore, the requirement of regularity for the mass function, that it must vanish at the origin of the radial coordinate from physical considerations, leads to $m(r = 0) = 0$. On imposing (5b), one immediately writes Z in terms of the parameters appearing in the density assumption:

$$Z(r) = 1 - \left(\frac{\kappa\rho_c}{3}\right)r^2 + \left(\frac{\kappa\mu\rho_c}{5r_b^2}\right)r^4 =: 1 - br^2 + ar^4. \tag{7}$$

In contrast, Tolman's method was to assume the second form for Z (or equivalently for $\mathrm{e}^{-\lambda}$) in (7), and then obtain the density function from (2a) directly by differentiation. The physical constants μ, ρ_c, and r_b occur frequently enough in the combinations shown above that the constants a and b as defined in (7) will be used when

convenient. The solution methods for solving the ODEs obtained from the Einstein equations, particularly those leading to the Tolman VII solution, have been given in multiple references [4, 8] and will not be reproduced here.

The complete Tolman VII solution is specified with the two functions (8) and (9) below, together with the previously given density function (4), and the metric function Z in equation (7):

$$Y(\xi) = c_1 \cos(\phi\xi) + c_2 \sin(\phi\xi), \tag{8}$$

where $\phi = \sqrt{a/4}$. The quantity ξ is a new radial variable whose explicit expression in terms of r is

$$\xi(r) = \frac{2}{\sqrt{a}} \coth^{-1}\left(\frac{1+\sqrt{1-br^2+ar^4}}{r^2\sqrt{a}}\right) \tag{9}$$

and it has been employed to simplify the expression of Y.

Now that the full solution for the metric functions is known, the pressure can be computed through the relation (10), obtained from a simple rearrangement and variable change of (3):

$$\kappa p(r) = 4\frac{\sqrt{Z}}{Y}\frac{\mathrm{d}Y}{\mathrm{d}\xi} - \frac{1}{r}\frac{\mathrm{d}Z}{\mathrm{d}r} - \kappa\rho. \tag{10}$$

This substitution results in a very complicated-looking expression for the pressure,

$$\kappa p(r) = \frac{4\phi[c_2\cos(\phi\xi) - c_1\sin(\phi\xi)]\sqrt{1-br^2+ar^4}}{c_1\cos(\phi\xi)+c_2\sin(\phi\xi)} - 4ar^2 + 2b - \kappa\rho_c\left[1-\mu\left(\frac{r}{r_b}\right)^2\right]. \tag{11}$$

So far the two integration constants c_1 and c_2 appearing in the expression for Y, and therefore p, are completely arbitrary. Application of the the boundary conditions using equations (10), (5a), and (5b) leads to

$$\kappa(p+\rho)|_{x=x_b} = \frac{4\cancel{\sqrt{Z(x_b)}}}{\cancel{Y(x_b)}}\left.\frac{\mathrm{d}Y}{\mathrm{d}\xi}\right|_{\xi=\xi_b} - 2\left.\frac{\mathrm{d}Z}{\mathrm{d}x}\right|_{x=x_b}, \tag{12}$$

where $x \coloneqq r^2$ is another radial coordinate, and all the b-subscripted variables are the values at the boundary $r = r_b$. The cancellation shown results from matching to the exterior Schwarzschild solution. However, according to the second boundary condition (5a), the pressure has to vanish at the boundary; therefore equation (12) simplifies to

$$\kappa\rho|_{x=x_b} = 4\left.\frac{\mathrm{d}Y}{\mathrm{d}\xi}\right|_{\xi=\xi_b} - 2\left.\frac{\mathrm{d}Z}{\mathrm{d}x}\right|_{x=x_b},$$

which can be further simplified and rearranged as

$$\left.\frac{\mathrm{d}Y}{\mathrm{d}\xi}\right|_{\xi=\xi_b} = \frac{b-ax_b}{4} = \frac{\kappa\rho_c}{4}\left(\frac{1}{3}-\frac{\mu}{5}\right) =: \alpha. \tag{13}$$

Since the ODE, equation (2c) for Y, is second order, a second condition is required. This is simply going to be condition (5b) restated as

$$\begin{aligned} Y(x=x_b) &= \sqrt{1-bx_b+ax_b^2} \\ &= \sqrt{1-\kappa\rho_c r_b^2\left(\frac{1}{3}-\frac{\mu}{5}\right)} =: \gamma \end{aligned} \tag{14}$$

The two equations (13) and (14) constitute the complete Cauchy's boundary condition on Y. The integration constants c_1 and c_2 can now be determined from the simultaneous equations:

$$\begin{aligned} \left.\frac{\mathrm{d}Y}{\mathrm{d}\xi}\right|_{\xi=\xi_b} &= \phi\left[c_2\cos(\phi\xi_b) - c_1\sin(\phi\xi_b)\right] = \alpha, \\ &\therefore c_2\cos(\phi\xi_b) - c_1\sin(\phi\xi_b) = \alpha/\phi, \end{aligned} \tag{15}$$

$$\begin{aligned} Y(\xi=\xi_b) &= \gamma \\ &\therefore c_2\sin(\phi\xi_b) + c_1\cos(\phi\xi_b) = \gamma. \end{aligned} \tag{16}$$

This system can be solved by first multiplying (15) by $\cos(\phi\xi_b)$, and (16) by $\sin(\phi\xi_b)$, and adding the equations obtained, yielding c_2. Similarly, switching the multiplicands and performing a subtraction instead yields c_1, and these can be given in the form,

$$c_1 = \gamma\cos(\phi\xi_b) - \frac{\alpha}{\phi}\sin(\phi\xi_b), \tag{17}$$

$$c_2 = \gamma\sin(\phi\xi_b) + \frac{\alpha}{\phi}\cos(\phi\xi_b). \tag{18}$$

The integration constants are ultimately computed in terms of the parameter set $\mathbf{\Pi}$, and in doing so this completes the specification of the full Tolman VII solution in the new constant scheme.

An important quantity to consider (since it establishes whether or not the solution is relativistically causal) is the adiabatic speed of sound waves in the fluid. The usual definition of this quantity in perfect fluids is $v^2 = \mathrm{d}p/\mathrm{d}\rho$. However, it will be convenient to find an expression for the sound speed directly from the differential equations, since the expression and functional form while completely equivalent is simpler to work with. First, from the expression for the density (4), one obtains the derivative

$$\frac{\mathrm{d}\rho}{\mathrm{d}r} = -\frac{2\mu\rho_c}{r_b^2}r,$$

which is zero only at $r = 0$. For the other equation, the conservation of the energy-momentum tensor $\nabla_i T^i{}_j = 0$ reduces to

$$\frac{\mathrm{d}p}{\mathrm{d}r} = -\frac{\nu'(p+\rho)}{2} = -\frac{(p+\rho)}{Y}\frac{\mathrm{d}Y}{\mathrm{d}r}, \tag{19}$$

in the $j = 0$ case. These two expressions can be used to find $\mathrm{d}p/\mathrm{d}\rho$ for every value of r but the center, so that

$$v^2 = \frac{\mathrm{d}p}{\mathrm{d}\rho} = \left(\frac{\mathrm{d}p}{\mathrm{d}r}\Big/\frac{\mathrm{d}\rho}{\mathrm{d}r}\right) = \frac{r_b^2(p+\rho)}{2\mu\rho_c r Y}\frac{\mathrm{d}Y}{\mathrm{d}r}. \tag{20}$$

Using the expressions for all the terms in this formula, one obtains a relatively simple expression for the speed of sound.

The bulk modulus K of a fluid is a measure of the resistance of a fluid to change its volume under an applied pressure. For perfect fluids it is related to the speed of sound in the media through $K = \rho v^2$. This is also a quantity which may be computed for the fluid in the interior. This calculation demonstrates that the order of magnitude of the bulk modulus is significantly higher than any currently known substance by many orders of magnitude.

The next step to understanding this solution is to investigate the behavior of the solution as the parameter set is varied. The particular choice of parameters will be those that are associated with what one might expect for realistic compact astrophysical objects. As a result, central densities $\rho_c \sim 10^{15}\mathrm{g}\cdot\mathrm{cm}^{-3}$ will be typical. Similarly, radii $r_b \sim 10^6\mathrm{cm}$ (i.e. 10 km) will often be used for the same reason. As stated above, the density profile (4) will decrease quadratically, and this provides a good approximation of what one would expect from a number of neutron star EOSs. Figure 1 plots the density as a function of radius for different values of μ, which controls the relation of the surface density to the central density.

The surface density ranges from a zero value when $\mu = 1$ to increasingly higher densities as μ is decreased. In the literature [13], models having zero surface densities have been called "natural," and those with nonvanishing surface densities have been called "self-bound." It is for this reason that μ is called the "self-boundedness" parameter.

Similarly, the complicated expression for the pressure given by equations (11), (17) and (18) can also be plotted as a function of the radius. Of importance here is the fact that while the densities might not vanish at the boundary r_b, the pressure for all parameter values must do so according to the boundary condition (5a). This is eminently clear in Fig. 2, where we see the pressures associated with the density curves shown in Fig. 1. Similarly the speed of sound and bulk modulus, all associated with the matter content in the star are shown in Figs. 3 and 4 respectively.

The functions $Z(r)$ and $Y(r)$ representing the solutions to the differential equations (2) are given in Figs. 6 and 5 respectively, again for different values of the self-boundedness μ. Equivalently the metric coefficients in

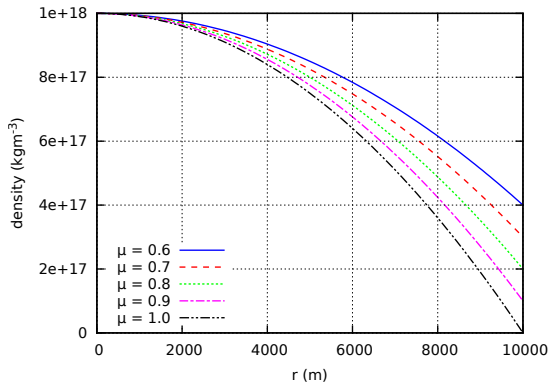

Figure 1. Variation of density with the radial coordinate inside the star. The parameter values are $\rho_c = 1\times10^{15}\mathrm{g}\cdot\mathrm{cm}^{-3}$, $r_b = 1\times10^6\mathrm{cm}$ and $0.6 \le \mu \le 1.0$.

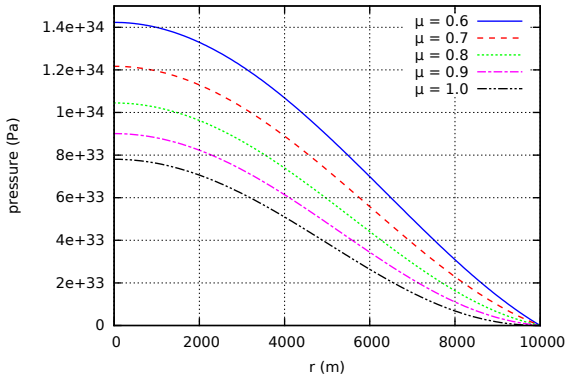

Figure 2. Variation of pressure with the radial coordinate inside the star. The parameter values are $\rho_c = 1\times10^{15}\mathrm{g}\cdot\mathrm{cm}^{-3}$, $r_b = 1\times10^6\mathrm{cm}$ and $0.6 \le \mu \le 1.0$.

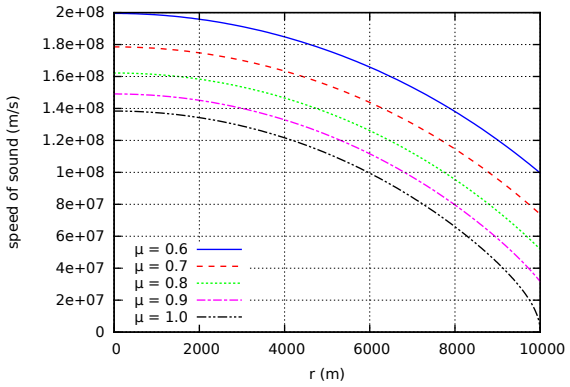

Figure 3. Variation of speed of sound with the radial coordinate inside the star. The parameter values are $\rho_c = 1\times10^{15}\mathrm{g}\cdot\mathrm{cm}^{-3}$, $r_b = 1\times10^6\mathrm{cm}$ and $0.6 \le \mu \le 1.0$.

Schwarzschild form: the form most often used in the literature for specifying static spherically symmetric models can be obtained from $Y(r)$ and $Z(r)$. For the sake of completeness, $\lambda(r)$ is plotted in Fig. 7 and $\nu(r)$ is plotted

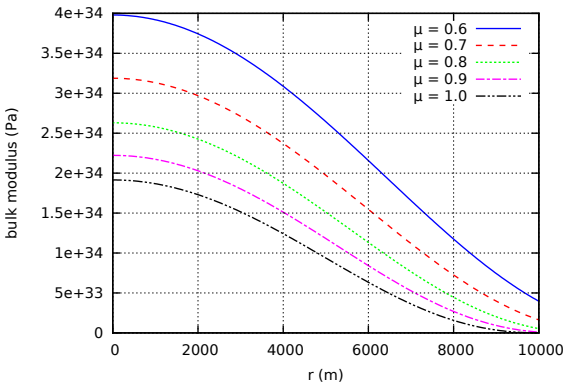

Figure 4. Variation of bulk modulus with the radial coordinate inside the star. The parameter values are $\rho_c = 1 \times 10^{15}\mathrm{g \cdot cm^{-3}}$, $r_b = 1 \times 10^6\mathrm{cm}$ and $0.6 \leq \mu \leq 1.0$.

in Fig. 8.

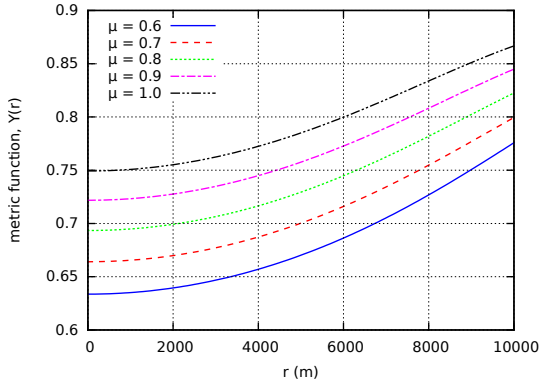

Figure 5. Variation of Y metric variable with the radial coordinate inside the star. The parameter values are $\rho_c = 1 \times 10^{15}\mathrm{g \cdot cm^{-3}}$, $r_b = 1 \times 10^6\mathrm{cm}$ and $0.6 \leq \mu \leq 1.0$. taking the various values shown in the legend.

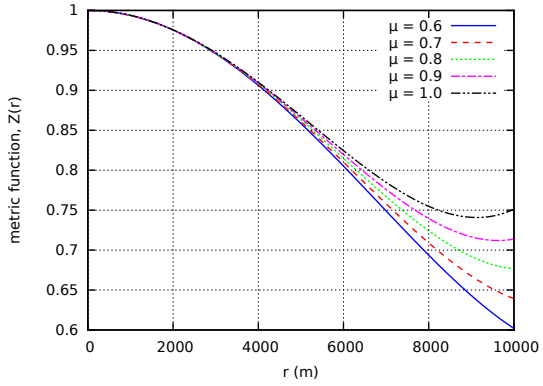

Figure 6. Variation of Z metric variable with the radial coordinate inside the star. The parameter values are $\rho_c = 1 \times 10^{15}\mathrm{g \cdot cm^{-3}}$, $r_b = 1 \times 10^6\mathrm{m}$ and $0.6 \leq \mu \leq 1.0$.

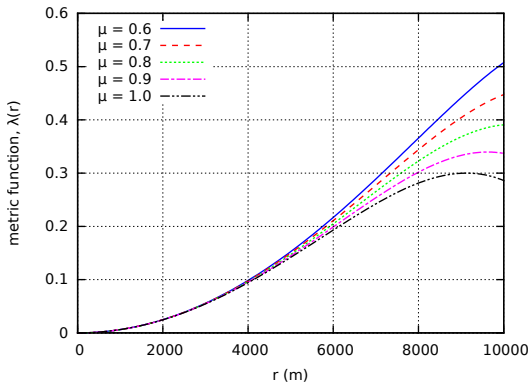

Figure 7. Variation of λ metric variable with the radial coordinate inside the star. The parameter values are $\rho_c = 1 \times 10^{15}\mathrm{g \cdot m^{-3}}$ $r_b = 1 \times 10^6\mathrm{cm}$ and $0.6 \leq \mu \leq 1.0$.

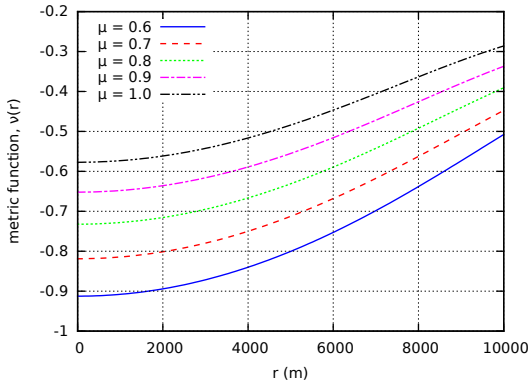

Figure 8. Variation of ν metric variable with the radial coordinate inside the star. The parameter values are $\rho_c = 1 \times 10^{15}\mathrm{g \cdot cm^{-3}}$ $r_b = 1 \times 10^6\mathrm{m}$ and $0.6 \leq \mu \leq 1.0$.

The redshift z_s of light emanating from a star as perceived by distant observers is another quantity that potentially can be measured. This quantity can also be calculated in our model, from the relation

$$z_s = \left(1 - \frac{2m(r_b)}{r_b}\right)^{-\frac{1}{2}} - 1.$$

The redshift value at the surface of the star for different values of μ is shown in Fig. 9.

III. THE EQUATION OF STATE AND PHYSICAL MODELS

A nice feature of the density assumption (4) is that it can be inverted to easily obtain r as a function of ρ. This allows one to generate an equation of state (EOS) for this solution. The full equation of state is given below:

$$p(\rho) = -\frac{1}{20\pi h_1 h_2}\left\{h_1 - h_2\sqrt{-2f_1\cot^2 f_2} + 4\pi h_1 h_2 \rho\right\},$$

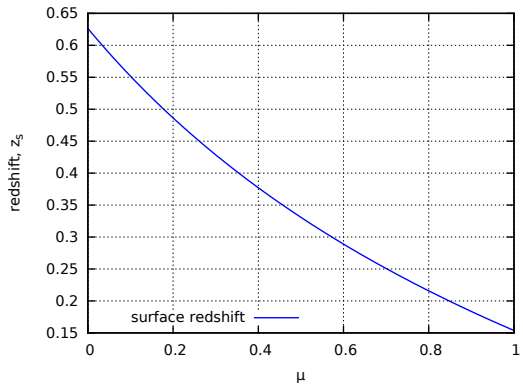

Figure 9. The redshift z_s at the surface of the sphere for different values of μ.

where $f_1(\rho)$ and $f_2(\rho)$ are functions of the density:

$$f_1(\rho) = 50 - 3\left(\frac{h_1}{h_2}\right)^2 - \frac{4\pi h_1^2}{h_2}\rho + 32\pi^2 h_1^2\rho^2$$

and

$$f_2(\rho) = \frac{1}{2}\ln\left[\frac{\sqrt{8f_1h_2} + h_1 - 16\pi h_1 h_2\rho}{20h_2C}\right].$$

The constants h_1 and h_2 are determined by the central density and μ, as follows:

$$h_1 = r_b\sqrt{\frac{5}{2\pi\rho_c\mu}} \qquad \text{and} \qquad h_2 = \frac{3}{8\pi\rho_c},$$

while the constant C is expressible as a complicated function of the parameters only, in terms of the auxiliary variables σ and χ:

$$C = \left(1 - \frac{h_1}{4h_2}\right)\sqrt{\frac{h_1(4h_2 - h_1)}{8r_b^2h_2 - h_1^2 + \chi}}\exp\left[\arctan\left(\frac{\chi}{\sigma}\right)\right],$$

with

$$\chi = 4\sqrt{h_2(4h_2r_b^4 - h_1^2r_b^2 + h_1^2h_2)},$$
$$\sigma = 16h_2r_b^2 + 8\pi\rho_c h_1^2h_2(1-\mu) - 2h_1^2.$$

It should be noted here that no assumption about the nature of matter, except for the very general thermodynamic prescription of a perfect fluid, has gone into this solution. Everything else, and in particular the equation of state, was obtained solely by virtue of the field equations and the density profile (4). With the equation of state now given explicitly as $p = p(\rho)$, it is a simple matter to find the derivative $\mathrm{d}p/\mathrm{d}\rho$ for the speed of pressure waves, and this yields precisely the same function as the one found previously in equation (20).

The expression for this class of EOS is somewhat complicated, but it is not without physical interpretation, contrary to what Tolman [4] thought in 1939:

> The dependence of p on r, with $\mathrm{e}^{-\lambda/2}$ and $\mathrm{e}^{-\nu}$ explicitly expressed in terms of r, is so complicated that the solution is not a convenient one for physical considerations.

By virtue of having a class of exact EOS, there is the possibility of two separate interpretations for an EOS that arise from the analytic expressions. This classification can be seen as a practical way of interpreting a class of EOS that has four different parameters, not all independent of each other. Both $p(\rho;\mathbf{\Pi})$ for $\rho_b = \rho_c(1-\mu) \le \rho \le \rho_c$, with the values of the elements of $\mathbf{\Pi}$, in particular ρ_c, fixed (henceforth called EOS1); and $p(\rho = \rho_c;\mathbf{\Pi})$, with the parameters of $\mathbf{\Pi}$ varying between limits imposed by causality (EOS2), could be candidates of the EOS.

In the literature, both interpretations have been used, and sometimes even interchanged. However, each has a completely different content in that the first interpretation expresses how the pressure of the fluid changes in moving from the center of the star $r = 0, \rho = \rho_c$, to the boundary $r = r_b, \rho_b = \rho_c(1-\mu)$, while all the integration constants, and hence parameters $\mathbf{\Pi}$, are kept fixed. Those seeking an interpretation of a unique EOS that should be applicable to all neutron stars without exception would find this interpretation sufficient.

The second interpretation, by contrast, looks closely at the fluid material itself and how the pressure at a certain point in the star changes as the density of the fluid at the center changes. Given that the central mass density of a compact star is inaccessible, this interpretation is of interest to those who believe that the central density should be a free parameter in a neutron star model. This would allow one to explore the possibilities that such a parameter change has on the observable quantities of the stars.

At this point in the derivation, a causality condition has not been imposed upon expressions of EOS1 or EOS2. Therefore, the class of EOS obtained can take a wide range of parameter values, as long as the metric functions and derived curvature tensors do not have singularities. The conditions leading to such singularities are narrower than the causality criterion, and enforcing the latter ensures that the parameter values do not cause singular behavior in the solution, and hence the class of EOS.

We first carry out an analysis of EOS1, and find that, to a high degree of accuracy, the variation of $p(\rho;\mathbf{\Pi})$, with ρ, and equivalently r, is very close to that of a generalized polytrope of the general form $p = k\rho^\gamma - p_0$, where p_0 is a pressure constant chosen such that p vanishes when $\rho = \rho_b$ at the boundary of the star and, as usual,γ and k are the adiabatic index and the adiabatic constant, respectively. This relation is very obvious from the shape of the curve in the "natural" $\mu = 1$ case as is seen in the one curve in Fig. 10, and all the curves in Figs. 12 and 13. It is interesting to note that the $\mu < 1$ cases all show a behavior similar to that found for other self-bound EOSs. (See e.g. Fig. 1 in the review by Lattimer and Prakash [13]). Indeed, Fig. 13 even seems to suggest

that varying the boundary radius r_b changes the value of k in the polytrope, and Fig. 12 that varying ρ_c changes the value of γ in the polytrope.

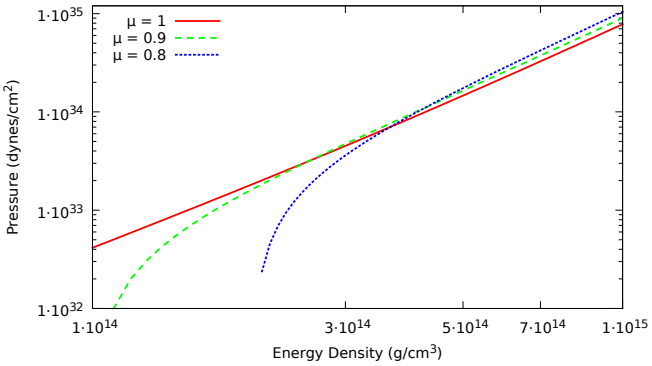

Figure 10. Log-log plot of pressure versus density for neutron star models determined by different μ, but the same ρ_c and r_b. The densities and pressures are in cgs units, and the $\mathbf{\Pi}$ is fixed by the following: $r_b = 10^6$cm, $\rho_c = 10^{15}\mathrm{g}\cdot\mathrm{cm}^{-3}$. Since pressure is a decreasing function of distance from the center, large densities indicate points closer to the center of the star.

Models employing polytropic perfect fluids use similar values for the adiabatic index γ as what we find for a range of different values of parameters $\mathbf{\Pi}$. This is shown in Fig. 11 which treats γ as a continuous variable defined by $\gamma = \frac{\mathrm{d}(\log p)}{\mathrm{d}(\log \rho)}$, and can be understood as the slope of the previous log-log graph.

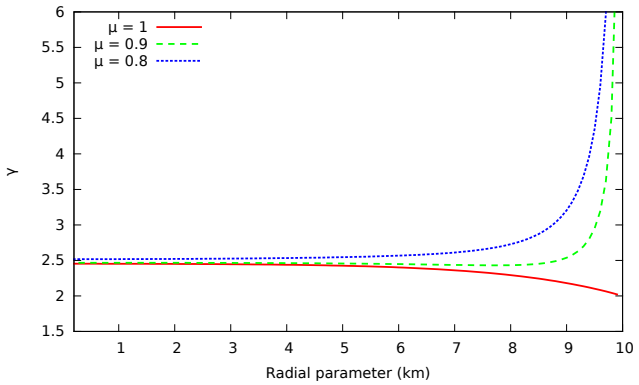

Figure 11. The adiabatic index variation from the center to the boundary of the star for different values of the parameter μ. The other parameter values are the same as those in Fig. 10.

From this figure it becomes evident how both types of stars have an interior structure well described by a polytrope with an adiabatic index close to 2.5. The "self-bound" stars exhibit the existence of an envelope consisting of material that is considerably stiffer than that found in the interior. Physically this is intuitive: for fixed ρ_c and r_b, the self-bound stars will become more and more massive as μ decreases. The increasing boundary density discontinuity requires a stiffer exterior mass distribution to maintain the hydrostatic equilibrium condition.

A notable characteristic of the class of EOS is its uncanny ability to distinguish between the different types of matter that make up the natural and the self-bound stars. Since the mass density (4) is a monotonically decreasing function of stellar radius, Fig. 11 can be thought of as the equivalent of a "flipped" and "rescaled" plot of the adiabatic index as a function of density. For the case $\mu = 1$, Figs. 10 and 11 are consistent with a number of hadronic EOS proposals. For densities in the range of $1\text{-}10\times10^{14}\mathrm{g}\cdot\mathrm{cm}^{-3}$ the adiabatic index ranges from 2.7 for the most dense nuclear material to 2.0 for the lower-density material. This type of behavior is found, for example, in a model proposed byGlendenning[16], that consists of a mixture of baryons.

For the self-bound models, where $\mu < 1$, the Tolman EOS is consistent with quark models using the MIT bag model. Fig. 10 is similar in nature to the strange quark models (SQM1-3) shown in Fig. 1 in [13] while Fig. 11 has similarities to the work of Casali and Menezes, who analyze the MIT bag model (see also the book by Haensel *et al.* [18]) and where it is found that the EOS for quark matter stiffens significantly at low densities [17]. The adiabatic index of that material reaches very high values (e.g. $\gamma > 7$ for densities less than 10^{14} $\mathrm{g}\cdot\mathrm{cm}^{-3}$).

To fully understand the nature of the EOS, the effect on the matter resulting from changing the other two parameters of $\mathbf{\Pi}$ can be investigated. Figure 12 demonstrates how the EOS inside the star changes as the central density ρ_c changes, and similarly Fig. 13 shows how the EOS varies with changes in the magnitude of the boundary radius r_b.

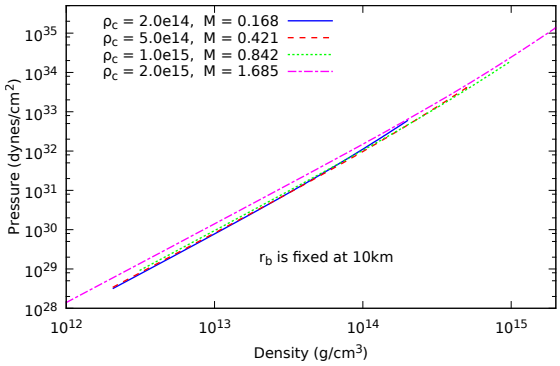

Figure 12. The effect of changing the central density ρ_c through 1 order of magnitude on the EOS with a boundary radius kept fixed at 10 km, for the natural EOS with $\mu = 1$. We notice that the slopes of the lines change by very little. The legend also provides the corresponding masses associated with each parameter choice in solar mass units.

What these figures show is that the value of the free parameters can change by up to an order of magnitude, yielding drastically different masses, while maintaining the same general polytropic behavior, *independently* of the parameter choices. At the highest densities, Fig. 12

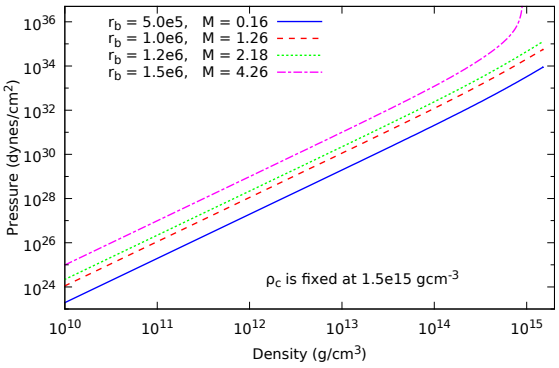

Figure 13. The effect of changing the boundary radius r_b through 1 order of magnitude, while the central density is kept fixed at 1.5×10^{15} g $\cdot$ cm^{-3}. We notice that the lines remain mostly parallel, suggesting that only the k value in the polytrope is changing, while the adiabatic index is remaining about the same. The masses of the corresponding stars are also provided in solar units in the legend.

shows that the EOS are nearly independent of the central density parameter. Figure 13 which demonstrates how the EOS changes under changes in the boundary radius, indicates that the adiabatic index γ is fixed over a large range of densities, but as expected the adiabatic constant k is different for different stars. The self-boundedness parameter μ, however, changes the character of this polytrope very much, as is clear in Fig. 11, hinting that the same EOS can have a richer structure than can be ultimately specified by the central density alone.

This polytropic behavior is very satisfying, since we started by trying to model a relativistic star from a Newtonian picture. That a class of EOS globally similar to the solutions of the Lane-Emden equations becomes apparent when we extend the nonphysical Schwarzschild interior to a more realistic density profile suggests that Tolman VII is at least as good as the Newtonian neutron stars, however with relativity being taken into account.

Now turning to the second way to characterize the class of EOS, concentrating on the behavior of the fluid material itself, independent of the geometry of the star, we determine how different physical quantities depend on the values of the central density ρ_c. The total mass-energy is defined as

$$M = 4\pi \int_0^{r_b} \bar{r}^2 \rho(\bar{r}) \mathrm{d}\bar{r} = \frac{4\pi r_b^3 \rho_c \,(5 - 3\mu)}{15}. \qquad (21)$$

The mass is important, since it is the only directly and reliably measurable quantity that can be obtained from neutron star observations. Lattimer and Prakash[13, 19, 20] and others [21, 22] have ruled out certain EOS2 based on mass and spin measurement of neutron stars. The former have also used Tolman VII, to constrain other EOS2 based on nuclear microphysics, and have even postulated that Tolman VII could be used as a guideline discriminating between viable and nonviable EOS2 [20]. If this postulate is true, given that the complete Tolman VII EOS2 is known, the condition that the solution must be causal can be applied, independent of measurements first, and then compared with the previous works [20, 22].

This is done in Fig. 14, where we superimpose the result of Ref. [22], on our own analysis of the whole solution space $\mathbf{\Pi}$. The surface shown is that for the values at which the speed of sound $v_s = \left(\sqrt{\mathrm{d}p/\mathrm{d}\rho}\right)\Big|_{r=0}$ at the center of the fluid sphere just reaches the speed of light. This is a sufficient condition for the solution to be causal, since v_s is a monotonically decreasing function of r in the sphere. Any point located below this surface has coordinate values for M, ρ_c, and μ that represent a valid *causal* solution to the Tolman VII differential equations. The orange line is the previous result obtained by Glendenning [22] from rotational considerations.

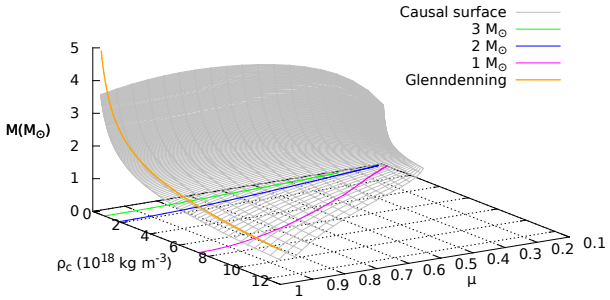

Figure 14. The mass of possible stars just obeying causality. The grey surface obeys the equation $v_s(r = 0) = \mathrm{c}$. Every point below the surface is a possible realization of a star, and we can potentially read off the mass, central density, and μ value of that star. The numbered lines represent stars with the same mass that are causal, i.e. they are projections of the causal surface onto the ρ_c-μ plane. Glendenning's [22] curve is shown in orange and represents a limit in the natural case only, and according to our results is acausal, being above our surface. The $\mu = 1$ plane's intersection with our graph is the graph given in Ref. [20], and here too our prediction is more restrictive.

Imposing causality to constrain the parameter space $\mathbf{\Pi}$ is not a new idea. However, having an explicit EOS allows one to easily generate the causal surface shown in Fig. 14, exactly without having to do any numerical gymnastics to find the speed of sound.

One method often used to distinguish between different EOS2 has been to calculate the compactness ratio, given by $\beta = \frac{GM}{c^2 r_b}$. In the case of Tolman VII the values of β for a large range of parameter variations $\mathbf{\Pi}$ are relatively constant. This means that even though we might change the value for $\mathbf{\Pi}$ of the stars, the ones bordering on causality share very similar compactness, albeit one that is lower than that previously thought possible. We show how this compactness β varies with μ in Fig. 15. Clearly the variation of β is small ($0.27 < \beta < 0.29$) over a large

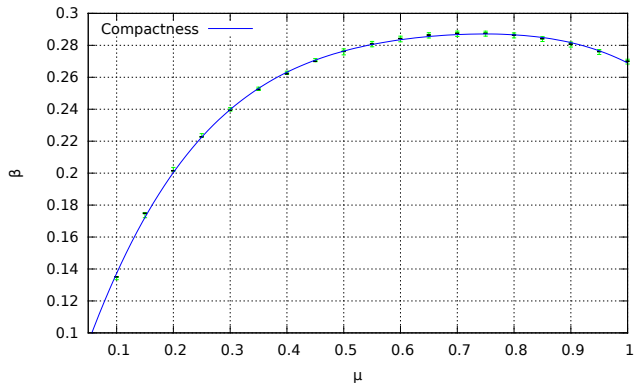

Figure 15. The compactness as a function of the self-boundedness parameter μ. This plot was generated by varying r_b from 4 km to 20 km for fixed μ and finding ρ_c and subsequently the compactness each time, such that the sound speed was causal at the center of the star. The curve shown is a polynomial fit, and the box-and-whisker plots(very small in green) show the variation of β for fixed μ, but different r_b. The very small whiskers justify the pertinence of β as a useful measure in the analysis of the behavior of the model.

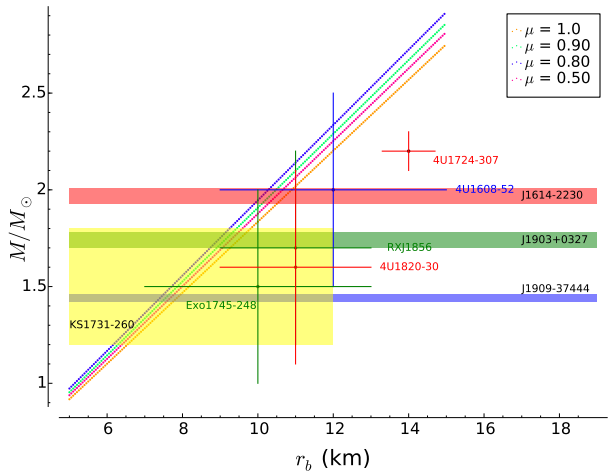

Figure 16. The mass M in solar units versus radius r_b in kilometers of a few stars for which these values have been measured. We use error bars to denote observational uncertainties, and colored bands in the case where only the mass is known. The lines we show and the ones that are at the causality limit in the Tolman VII model, and the whole area below those lines can be causal parameter choices for stars.

range of values for μ ($0.45 < \mu < 1.0$). A value for the maximal compactness of about 0.34 from rotational and causality criteria was obtained by Ref. [20]. Our analysis shows that β is less than 0.3 for all possible stars, if Tolman VII is a valid physical model (at least as a limit) for stars. Recently radius measurements of a limited number of neutron stars have been obtained [23–26]. These are shown along with some other stars of known mass in Fig. 16. We also superimpose a few of the limiting causal curves obtained for different values of μ from Tolman VII, to show that Tolman VII is not ruled out by observational results, even though it predicts lower compactness than most nuclear models. The dotted lines shown in the figure represent the causal limits for different values of the self-boundedness parameter μ.

For a fixed value of μ, causality requirements determine the relationship between the central density and the boundary of the star. A typical M-R curve for a particular EOS2 would be determined by fixing the parameters associated with a particular EOS2 and then computing the mass as a function of the star's radius. All possible curves of this nature lie to the right of the curves shown in Fig. 16 and thus any curves in that region represent a viable model for neutron star structure obtained from a Tolman VII solution. This is one advantage of having a complete analytic solution to the Einstein equations. Rather than integrate (using numerical methods) the TOV equation for a specific set of EOS parameters, an entire class of solutions are provided by the complete analytic expressions. Physical constraints on the solution (such as causality) then provide restrictions on that class of solutions. What the curves shown in this plot represent are the maximum possible cases for the (M, r_b) relation provided by the causal Tolman VII EOS solutions. Therefore, the whole space to the right of those lines can potentially yield a causal EOS and thus Fig. 16 shows that Tolman VII is not ruled out yet as a viable model for compact objects unless the radii of some of the neutron stars with known masses are so small that they would be represented by a point to the left of the curves.

The lines shown are on the edge of causality in the following way: the speed of sound, a monotonically decreasing function of the radius, is just equal to the speed of light at the center where $r = 0$– that is, the lines are the counterparts of those points that make up the surface of Fig. 14. Since all observations of compactness are bounded by the most extreme Tolman VII model, we claim that the solution may actually realized by compact stars in nature.

IV. CONCLUSION

A complete analysis of the Tolman VII solution has been carried out, and it was found that it is a physically valid solution with a huge potential for modeling physical objects. The class of EOS this solution predicts has been found, and in certain regimes behaves very much like a polytrope with an adiabatic index of 2.5, independently of the choices of two parameters: the central density and the radius of the star. The third parameter, the self-boundedness, changes the polytropic index drastically, particularly at the edge of the star, as expected from a naive Newtonian approach to stellar structure. That this solution has a density profile that is very close to the hand-picked, but thermodynamically motivated polytropes of Newtonian stars, while still being a full

relativistic model is a very good reason to take its predictions of stellar structure seriously.

It is also interesting that the type of matter that produces the different EOSs depends crucially on the value of μ. Hadronic matter is obtained with $\mu = 1$, while $\mu < 1$ stars would appear to be made up of quark matter.

Using the EOS derived from Tolman VII, we are able to compute the speed of pressure waves, and imposing causality on the latter results in a more restrictive limit on the maximum compactness of fluid spheres allowable by classical general relativity. This is possible to do without the use of numerical computations because of the exact form of the class of EOSs generated by the quadratic density falloff assumption in Tolman VII.

The solution is, moreover, stable under radial perturbations, since the speed of these pressure waves is finite and monotonically decreasing from the center outwards, thus satisfying the stability criterion in Ref. [27]. If we believe as in Ref. [20] that Tolman VII is an upper limit on the possible energy density ρ_c, for a given mass M, some known models [19] which predict higher compactness than Tolman VII will have to be reconsidered, since they still maintain a quadratic density profile to first order, and thus cannot also be causal at these higher compactnesses.

[1] D. Kramer, H. Stephani, M. A. H. MacCallum, and E. Herlt, *Exact solutions of Einstein's field equations* (Deutscher Verlag der Wissenschaften, Berlin, and Cambridge University Press, Cambridge, 1980) pp. 1–425, 1.2.

[2] M. S. R. Delgaty and K. Lake, "Physical acceptability of isolated, static, spherically symmetric, perfect fluid solutions of Einstein's equations," Computer Physics Communications **115**, 395–415 (1998).

[3] M. R. Finch and J. E. F Skea, "A review of the relativistic static sphere," (1998), unpublished, available at `www.dft.if.uerj.br/usuarios/JimSkea/papers/pfrev.ps`.

[4] R. C. Tolman, "Static Solutions of Einstein's Field Equations for Spheres of Fluid," Physical Review **55**, 364–373 (1939).

[5] W. Kinnersley, "Recent Progress in Exact Solutions," in *Relativity and Gravitation*, edited by G. Shaviv and J. Rosen (1975) p. 109.

[6] M. C. Durgapal and G. L. Gehlot, "Spheres with varying density in general relativity," Journal of Physics A: General Physics **4**, 749–755 (1971).

[7] M. C. Durgapal and P. S. Rawat, "Non-rigid massive spheres in general relativity," Mon. Not. R. Astron. Soc. **192**, 659–662 (1980).

[8] A. L. Mehra, "Radially symmetric distribution of matter," Journal of the Australian Mathematical Society **6**, 153–156 (1966).

[9] N. Neary and K. Lake, "r-modes in the Tolman VII solution," ArXiv General Relativity and Quantum Cosmology e-prints (2001), gr-qc/0106056.

[10] Nicholas Neary, Mustapha Ishak, and Kayll Lake, "The Tolman VII solution, trapped null orbits and w - modes," Physical Review D **64**, 084001 (2001).

[11] G.P. Horedt, *Polytropes: Applications in Astrophysics and Related Fields*, Astrophysics and Space Science Library (Springer Netherlands, 2004).

[12] H. A. Buchdahl, "General relativistic fluid spheres," Phys. Rev. **116**, 1027–1034 (1959).

[13] J. M. Lattimer and M. Prakash, "Neutron Star Structure and the Equation of State," The Astrophysical Journal **550**, 426–442 (2001), in particular Fig. 5 shows the quadradic fall-off behaviour of the density.

[14] B. V. Ivanov, "Static charged perfect fluid spheres in general relativity," Physical Review D **65**, 104001 (2002).

[15] J.L. Synge, *Relativity: the general theory*, Series in physics (North-Holland Pub. Co., 1960).

[16] N. K. Glendenning, "Neutron stars are giant hypernuclei?" ApJ **293**, 470–493 (1985).

[17] R. H. Casali and D. P. Menezes, "Adiabatic index of hot and cold compact objects," Brazilian Journal of Physics **40**, 166 – 171 (2010).

[18] P. Haensel, A.Y Potekin, and D.G Yakovlev, *Neutron Stars 1 : Equation of State and Structure*, Vol. 1 (Springer, 2007).

[19] J. M. Lattimer and M. Prakash, "Neutron star observations: Prognosis for equation of state constraints," Phys. Rep. **442**, 109–165 (2007).

[20] James M. Lattimer and Madappa Prakash, "Ultimate energy density of observable cold baryonic matter," Phys. Rev. Lett. **94**, 111101 (2005).

[21] Norman K. Glendenning, "First-order phase transitions with more than one conserved charge: Consequences for neutron stars," Phys. Rev. D **46**, 1274–1287 (1992).

[22] N. Glendenning, *Compact Stars. Nuclear Physics, Particle Physics and General Relativity.* (Springer-Verlag New York, 1996).

[23] Feryal Özel, Tolga Güver, and Dimitrios Psaltis, "The mass and radius of the neutron star in exo 1745248," The Astrophysical Journal **693**, 1775 (2009); Feryal Özel and Dimitrios Psaltis, "Reconstructing the neutron-star equation of state from astrophysical measurements," Phys. Rev. D **80**, 103003 (2009); Tolga Güver, Patricia Wroblewski, Larry Camarota, and Feryal Özel, "The mass and radius of the neutron star in 4u182030," The Astrophysical Journal **719**, 1807 (2010); T. Güver, F. Özel, A. Cabrera-Lavers, and P. Wroblewski, "The Distance, Mass, and Radius of the Neutron Star in 4U 1608-52," ApJ **712**, 964–973 (2010).

[24] F. Özel, A. Gould, and T. Güver, "The Mass and Radius of the Neutron Star in the Bulge Low-mass X-Ray Binary KS 1731-260," ApJ **748**, 5 (2012).

[25] V. Suleimanov, J. Poutanen, M. Revnivtsev, and K. Werner, "A Neutron Star Stiff Equation of State Derived from Cooling Phases of the X-Ray Burster 4U 1724-307," ApJ **742**, 122 (2011).

[26] A. W. Steiner, J. M. Lattimer, and E. F. Brown, "The Equation of State from Observed Masses and Radii of Neutron Stars," ApJ **722**, 33–54 (2010).

[27] H. Abreu, H. Hernández, and L. A. Núñez, "Sound speeds, cracking and the stability of self-gravitating anisotropic compact objects," Classical and Quantum

Gravity **24**, 4631–4645 (2007).